Insights into Male Androgenetic Alopecia: Differential Gene Expression Profiling of Plucked Hair Follicles and Integration with Genetic Data

JID Open

Journal of Investigative Dermatology (2019) **139,** 235–238; doi:10.1016/j.jid.2018.06.182

TO THE EDITOR

Male androgenetic alopecia (AGA) is a highly heritable disorder characterized by a distinct pattern of progressive scalp hair loss. To date, genome-wide association studies have identified more than 300 genome-wide significant AGA risk variants (Hagenaars et al., 2017; Heilmann-Heimbach et al., 2017). The majority are located in noncoding genomic regions, and the precise biological mechanisms through which they contribute to the key pathophysiological characteristics of AGA remain unclear (Heilmann-Heimbach et al., 2016). In genetic AGA research, a generally accepted hypothesis is that the functional effects of these noncoding variants are conferred through the tissue- and context-specific regulation of the expression of pathobiologically relevant genes. The key pathophysiological changes of AGA are limited to hair follicles (HFs) in the frontal and vertex regions of the scalp, with occipital scalp HFs being exempt. Improved understanding of the biological differences between HF populations that are prone to AGA compared with HF populations that are not prone to AGA is desirable and might contribute to the identification of genes and pathways of relevance to AGA pathobiology.

To pinpoint biological differences between HF subpopulations and to identify likely AGA candidate genes and pathways, we performed (i) a systematic investigation into the differential expression of micro(mi) RNAs and mRNAs in paired frontal and occipital plucked HFs (pHFs); and (ii) integration of these expression data with information on biological pathways and AGA genetic association data.

Paired pHFs from the frontal and occipital scalp were collected from 24 male donors (mean age: 24 years ± 1.4; Hamilton-Norwood grades I/II [87.5%] and III [12.5%]; Supplementary Table S1 online, Supplementary Figure S1 online). The study was approved by the ethics committee of the University of Bonn. Written informed consent was obtained from all study participants before inclusion.

The comparative analysis of expression profiles between frontal and occipital pHFs led to the identification of 143 differentially expressed (DE) miRNAs and 2,836 DE mRNAs ($P_{WMW} < 0.05$). Of these, 16 miRNAs and 37 mRNAs showed significant DE after the Benjamini-Hochberg correction ($P_{BH} < 0.05$, Figure 1, Supplementary Tables S2 and S3 online). These included (i) the mRNA genes *PER2*, *DLL1,* and *PAK1,* which have been implicated in the regulation of hair cycling, keratinocyte proliferation, and androgen signaling (Estrach et al., 2008; Plikus et al., 2013; Schrantz et al., 2004); and (ii) miR-1908-5p, whose target genes are enriched in the adipogenesis pathway implicated in the regulation of hair cycling and AGA (Kruglikov and Scherer, 2017). Although the majority of DE miRNAs ($P_{WMW} < 0.05$) showed lower expression levels in frontal pHFs (n = 124; 86.7%), the majority of DE mRNAs displayed higher expression levels in frontal pHFs (n = 1,915; 67.5%). This suggests that a loss of miRNA-mediated gene regulation may be implicated in the context-specific regulation of HF gene expression, and of relevance in terms of AGA development (Figure 1, Supplementary Tables S2 and S3).

To gain insights into the context-specific regulatory interactions of frontal and occipital pHFs, we tested for an enrichment of DE mRNAs ($P_{WMW} < 0.05$; n = 2,836) and target genes of the 16 significantly DE miRNAs in biological pathways. The pathway-based analysis for DE mRNAs identified 72 nominally significant pathways (Supplementary Table S4 online), 3 of which remained significant after correction for multiple testing ($P_{BH} < 0.05$). Of these, "ceramide biosynthesis" and "GADD45 signaling" are of potential relevance to AGA due to their reported role in the regulation of follicular homeostasis and apoptosis (Lin et al., 2017; Salvador et al., 2013). Target genes of the 16 significantly DE miRNAs were identified by (i) Spearman's rank correlation of pHF expressed miRNAs and mRNAs (Supplementary Table S5 online, n = 650); and (ii) extraction of pHF expressed, validated, and predicted target genes of these miRNAs from miRPathDB (n = 9,410). Subsequent pathway-based analysis of these target genes identified 187 pathways with $P_{BH} < 0.05$ that were targeted by at least 5 of the 16 DE miRNAs. These are likely to include pathways for which a loss of miRNA-mediated

Abbreviations: AGA, androgenetic alopecia; DE, differential expression/differentially expressed; HF, hair follicle; miRNA, microRNA; pHF, plucked hair follicle

Accepted manuscript published online 15 July 2018; corrected proof published online 25 September 2018

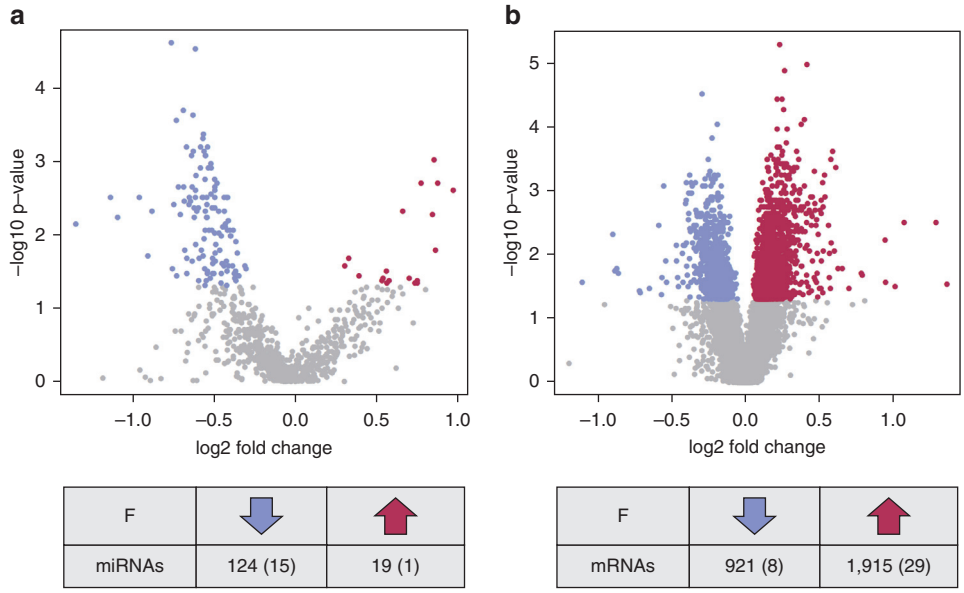

Figure 1. Volcano plots of the results of the differential microRNA (miRNA) and mRNA expression analyses. Each dot represents either (**a**) a plucked hair follicle (pHF) expressed mature miRNA (n = 823) or (**b**) a pHF expressed mRNA gene (n = 15,844). Differentially expressed genes at $P_{WMW} < 0.05$ are depicted in blue (frontal < occipital) and red (frontal > occipital). Arrows indicate up- (↑) or downregulation (↓) in frontal (F) tissue. Frontal upregulation was observed for 19 miRNAs and 1,915 mRNAs. Frontal downregulation was observed for 124 miRNAs and 921 mRNAs. Numbers in brackets denote the number of miRNAs and mRNAs that showed significant differential expression after the Benjamini-Hochberg correction for multiple testing ($P_{BH} < 0.05$).

regulation may be implicated in early AGA development (Supplementary Figure S2 and Table S6 online). These include previously associated pathways, such as WNT/β-catenin, androgen, estrogen, and melatonin signaling (Heilmann-Heimbach et al., 2017; Lolli et al., 2017), as well as pathways not previously reported in AGA. The latter included the ephrin-, ErbB-, and Hippo-signaling pathways, which have been implicated in HF growth and organ size regulation, processes of probable relevance to AGA (Wijeratne et al., 2016; Xie et al., 1999; Yu et al., 2015).

Next, we investigated whether the present DE data facilitated functional annotation and candidate gene identification at known AGA risk loci. A total of 100 DE mRNA and 6 DE miRNA genes were located at 57 known loci (Hagenaars et al., 2017; Heilmann-Heimbach et al., 2017) (Supplementary Table S7 online). These included promising candidate genes, such as the androgen receptor; the hair growth regulator *WNT3* (Millar et al., 1999); and *RORA*, a gene implicated in pelage density and hair regrowth (Steinmayr et al., 1998). Interestingly, a significant regulatory effect on *RORA* expression was found for the lead AGA single nucleotide polymorphism at 15q22.2 (rs2028122, Hagenaars et al., 2017), whereby AGA risk allele carriers showed significantly increased expression in frontal pHFs compared with nonrisk allele carriers ($P_{WMW} = 0.035$). Similar regulatory effects were detected for the lead AGA single nucleotide polymorphisms at (i) 1p12 (rs67803788, Hagenaars et al., 2017) on *FAM46C* and (ii) 21q22.12 (rs7280071, Heilmann-Heimbach et al., 2017; rs68088846, Hagenaars et al., 2017) on *RCAN1*. This suggests that the associated variants at these loci exert their functional effects in AGA via regulation of these candidate genes (Supplementary Figure S3 online).

Finally, we attempted to identify genomic regions for which involvement in AGA pathogenesis was suggested by both expression and genetic association data. Integration of the present gene expression data with previous AGA genetic association data (Hagenaars et al., 2017; Heilmann-Heimbach et al., 2017) led to the identification of seven genomic regions, six of which constitute previously unreported candidate regions for AGA ($P_{Perm} < 0.1$, Figure 2, Supplementary Table S8 online). One region on 3q22.2 ($P_{Perm} = 0.01$) is of particular interest. This region showed strong suggestive association with AGA in a large meta-analysis ($P = 9.1 \times 10^{-8}$, Heilmann-Heimbach et al., 2017), and includes the gene *EPHB1*, thus substantiating an involvement of ephrin signaling in AGA.

In conclusion, the present study identified a number of genes and pathways showing DE between pHF from different scalp areas. We generated evidence that a considerable fraction of these constitute promising candidates for AGA, because they have a probable contribution to (i) androgen sensitivity (*RORA, PAK1*); (ii) deregulation of HF growth or cycling (miR-1908-5p, ephrin receptor/B-signaling); or (iii) HF miniaturization (Hippo signaling). The study captured differences in gene expression in an easily accessible tissue of relevance to the phenotype. However, the use of pHF samples precluded insights into regulatory processes within other likely AGA-relevant tissues, such as the dermal papilla, the lower hair bulb epithelium, the bulge region, the arrector pili muscle, and the perifollicular environment. Moreover, we cannot entirely exclude the possibility that differences in cell composition, or cell number, between frontal and occipital pHFs, for example, due to the onset of miniaturization in

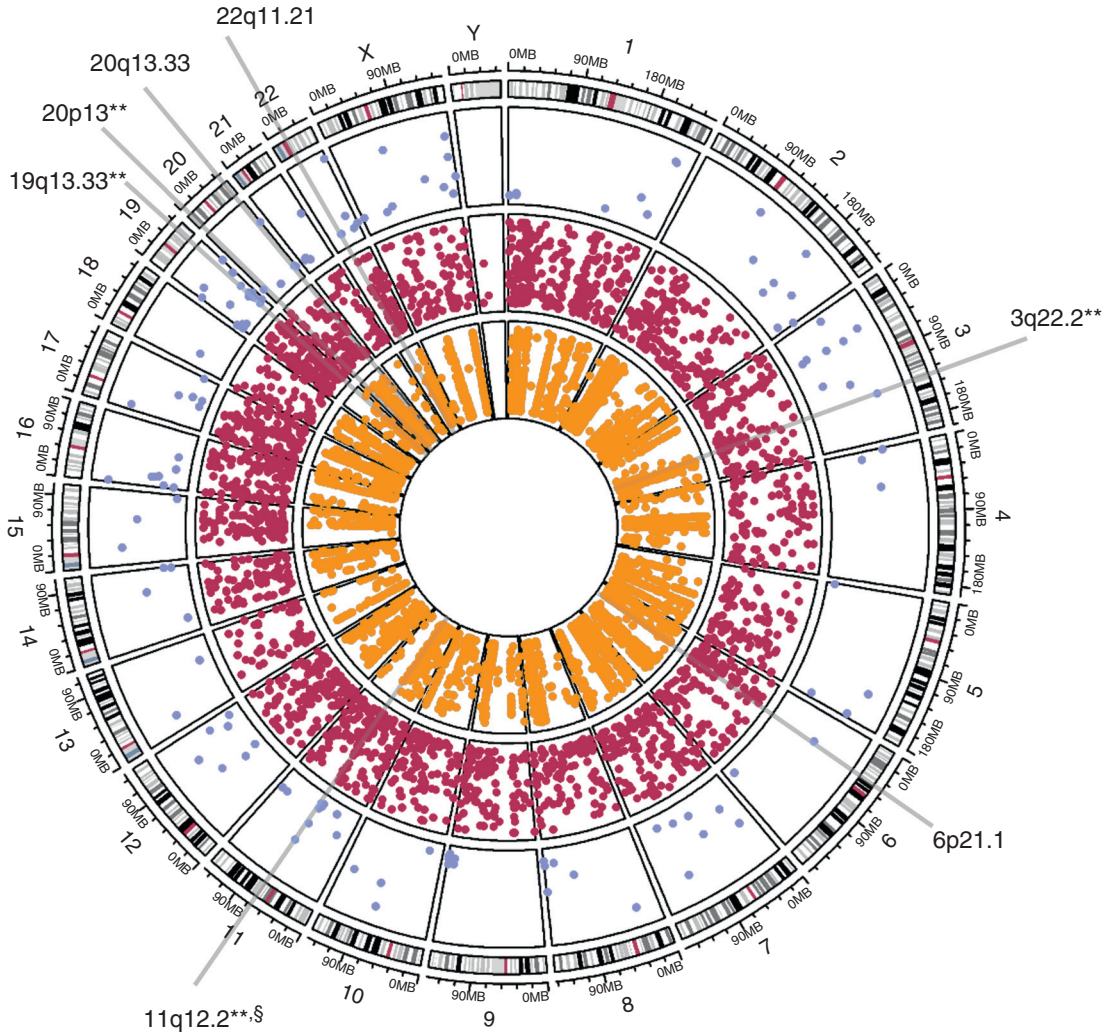

Figure 2. Integration of results of the present differential miRNA and mRNA expression profiling with previous AGA genetic association data. Circular plot showing the results of the integration of data on pHF miRNA (blue, outer circle) and mRNA (red, middle circle) differential expression with AGA genetic association data (green, inner circle) (Hagenaars et al., 2017; Heilmann-Heimbach et al., 2017). The analysis implicated seven genomic regions ($P_{Perm} < 0.1$) on chromosomes 3q22.2, 6p21.1, 11q12.2, 19q13.33, 20p13, 20q13.33, and 22q11.21. Six of these regions constitute previously unreported candidate regions for AGA. $^{**}P_{Perm} \leq 0.01$, §previously reported risk locus ($P < 5 \times 10^{-8}$, Hagenaars et al., 2017). AGA, androgenetic alopecia; miRNA, microRNA; pHF, plucked hair follicle.

frontal HFs, may have confounded our results. To substantiate the present findings and to elucidate the complex biological processes leading to AGA, future investigations should involve the analysis of paired HF samples from males across different age groups (prepubertal boys, elderly men); alternative sampling approaches; and refined analysis strategies, for example, single-cell transcriptomics and immune histochemical staining.

CONFLICT OF INTEREST

DAH, member of the MAAN consortium, is an employee of 23andMe (Mountain View, CA). The remaining authors state no conflict of interest.

ACKNOWLEDGMENTS

We thank the study participants for their cooperation. We also thank the employees of 23andMe for making this work possible and Christine Schmael for her critical reading of the manuscript. MMN is a member of the DFG Excellence Cluster ImmunoSensation. The study was supported by the BONFOR program of the Medical Faculty of the University of Bonn, Germany.

***Lara M. Hochfeld*[1,2], *Andreas Keller*[3], *Thomas Anhalt*[1,2], *Nadine Fricker*[1,2], *the Meta-analysis for Androgenetic Alopecia Novel determinants (MAAN) Consortium*[4], *Markus M. Nöthen*[1,2] *and Stefanie Heilmann-Heimbach*[1,2,*]**

[1]*Institute of Human Genetics, University of Bonn, School of Medicine & University Hospital Bonn, Bonn, Germany;* [2]*Department of Genomics, Life & Brain Center, University of Bonn, Bonn, Germany and* [3]*Chair for Clinical Bioinformatics, Saarland University, Saarbrücken, Germany*

[4]*MAAN consortium members and affiliation(s) are listed in the Supplementary Material online.*

[*]*Corresponding author e-mail: sheilman@uni-bonn.de*

SUPPLEMENTARY MATERIAL

Supplementary material is linked to the online version of the paper at www.jidonline.org, and at https://doi.org/10.1016/j.jid.2018.06.182.

REFERENCES

Estrach S, Cordes R, Hozumi K, Gossler A, Watt FM. Role of the Notch ligand Delta1 in embryonic and adult mouse epidermis. J Invest Dermatol 2008;128:825–32.

Hagenaars SP, Hill WD, Harris SE, Ritchie SJ, Davies G, Liewald DC, et al. Genetic prediction of male pattern baldness. PLOS Genet 2017;13:e1006594.

Heilmann-Heimbach S, Hochfeld LM, Paus R, Nöthen MM. Hunting the genes in male-pattern alopecia: how important are they, how close are we and what will they tell us? Exp Dermatol 2016;25:251–7.

Heilmann-Heimbach S, Herold C, Hochfeld LM, Hillmer AM, Nyholt DR, Hecker J, et al. Meta-analysis identifies novel risk loci and yields systematic insights into the biology of male-pattern baldness. Nat Commun 2017;165:1293–302.

Kruglikov IL, Scherer PE. Adipocyte-myofibroblast transition as a possible pathophysiological step in androgenetic alopecia. Exp Dermatol 2017;26:522–3.

Lin CL, Xu R, Yi JK, Li F, Chen J, Jones EC, et al. Alkaline ceramidase 1 protects mice from premature hair loss by maintaining the homeostasis of hair follicle stem cells. Stem Cell Reports 2017;9:1488–500.

Lolli F, Pallotti F, Rossi A, Fortuna MC, Caro G, Lenzi A, et al. Androgenetic alopecia: a review. Endocrine 2017;57:9–17.

Millar SE, Willert K, Salinas PC, Roelink H, Nusse R, Sussman DJ, et al. WNT signaling in the control of hair growth and structure. Dev Biol 1999;207:133–49.

Plikus MV, Vollmers C, La Cruz D de, Chaix A, Ramos R, Panda S, et al. Local circadian clock gates cell cycle progression of transient amplifying cells during regenerative hair cycling. Proc Natl Acad Sci USA 2013;110:E2106–15.

Salvador JM, Brown-Clay JD, Fornance AJ Jr. Gadd45 in stress signaling, cell cycle control, and apoptosis. Adv Exp Med Biol 2013;793:1–19.

Schrantz N, da Silva Correia J, Fowler B, Ge Q, Sun Z, Bokoch GM. Mechanism of p21-activated kinase 6-mediated inhibition of androgen receptor signaling. J Biol Chem 2004;79:1922–31.

Steinmayr M, Andre E, Conquet F, Rondi-Reig L, Delhaye-Bouchaud N, Auclair N, et al. staggerer phenotype in retinoid-related orphan receptor-deficient mice. Proc Natl Acad Sci USA 1998;95:3960–5.

Wijeratne DT, Rodger J, Wood FM, Fear MW. The role of Eph receptors and Ephrins in the skin. Int J Dermatol 2016;55:3–10.

Xie W, Chow LT, Paterson AJ, Chin E, Kudlow JE. Conditional expression of the ErbB2 oncogene elicits reversible hyperplasia in stratified epithelia and up-regulation of TGFalpha expression in transgenic mice. Oncogene 1999;18:3593–607.

Yu F-X, Zhao B, Guan K-L. Hippo pathway in organ size control, tissue homeostasis, and cancer. Cell 2015;163:811–28.

Enamel Anomalies in a Pachyonychia Congenita Patient with a Mutation in *KRT16*

Journal of Investigative Dermatology (2019) **139,** 238–241; doi:10.1016/j.jid.2018.07.005

TO THE EDITOR

KRT6A, *KRT6B*, *KRT6C*, *KRT16*, and *KRT17* genes encode a subset of epithelial keratins (K6a, K6b, K6c, K16, and K17) that are normally expressed in the skin of the palms and soles, in nail and hair, and in the oral epithelium. Mutations in these genes lead to pachyonychia congenita (PC), a cutaneous disorder featuring palmoplantar keratoderma and nail dystrophy, and potentially oral leukokeratosis, follicular keratosis, cysts, hyperhidrosis, and natal teeth (McLean et al., 2011; Smith et al., 2005; Wilson et al., 2011). In a recent study, we reported genetic association between common polymorphisms in *KRT6A*, *KRT6B*, and *KRT6C* and increased susceptibility to tooth decay (Duverger et al., 2018). We also showed that K6 proteins are produced by ameloblasts, highly specialized cells that drive the deposition of enamel rods and their maturation (Simmer et al., 2010), and are incorporated into the 1% protein fraction that persists into enamel after it is fully mineralized (Robinson et al., 1975). We further revealed structural enamel defects in a patient with PC carrying a p.Asn171Lys substitution in K6a (Duverger et al., 2018). The genetic association study did not allow us to draw any conclusion on the potential involvement of *KRT16* and *KRT17* in dental health due to a low number of polymorphisms that had high enough frequency in the cohorts studied. Here we report enamel defects in a patient with PC with a mutation in the *KRT16* gene.

In rodents, K16 is produced by secretory-stage ameloblasts and accumulates into the enamel matrix (Figure 1a). Outside the Tomes' processes, which correspond to the highly specialized apical end of the ameloblasts where enamel matrix deposition is coordinated, K16 was detected as parallel transverse bands within the enamel rods as well as in the interrod regions (Figure 1a, top inset). The persistence of K16 in mature human enamel was verified by immunostaining on polished sections of human third molars. K16 was detected in the inner portion of the enamel, close to the dentin-enamel junction where it stained the core of the enamel rods (Figure 1b), contrary to K6 proteins that tend to accumulate in the enamel rod sheaths located at the periphery of the rods (Duverger et al., 2018). The fact that K16 is detected in both rods and interrods during the process of enamel matrix deposition but found primarily in the enamel rods in mature enamel may be due to rearrangements happening during enamel maturation or to the masking of the epitope in the interrods of mature enamel.

The patient with PC introduced in this study, a female in her early twenties, was found to have a *KRT16 c.374A>G* mutation (Figure 1c) (Liao et al., 2007). This transition results in an asparagine to serine substitution at position 125 in the K16 protein, a substitution that falls at the beginning of the rod domain (Figure 1c). This patient had painful focal plantar keratoderma affecting weight-bearing areas of both soles and mild toenail dystrophy, which is commonly observed for this mutation (Figure 1d). Patient samples were obtained following written informed consent and ethical approval by a Western Institutional Review Board (Western IRB study no. 20040468) that complies with the Declaration of Helsinki. Permission to publish patient photographs was given.

As this patient underwent wisdom teeth extraction, we were able to perform thorough analysis of the

Abbreviations: ALC, ameloblast-like cell; PC, pachyonychia congenita

Accepted manuscript published online 15 July 2018; corrected proof published online 25 September 2018